A Bang-Bang Attitude Stabilizer for Rotating Rigid Bodies

Edoardo Serpelloni *, Manfredi Maggiore †

and Christopher J. Damaren‡

University of Toronto, Toronto, ON, M5S 2J7, Canada

In this paper we present a controller that solves the attitude control problem for an inertially symmetric rigid spacecraft with on-off thrusters. The proposed controller achieves the goal of attitude stabilization without inducing high-frequency switching of the thrusters. Each axis of the spacecraft is controlled independently by using a hybrid bang-bang controller originally designed for double-integrators. Simulations suggest that the proposed controller is robust with respect to external bounded perturbations.

I. Introduction

In this paper we consider the problem of stabilizing the orientation of a rigid body by means of bang-bang torques. Although many modern spacecraft are actuated using reaction wheels and control moment gyros providing a smooth control input, on-off jet thrusters still play a crucial role in performing reorientation maneuvers for large spacecraft. Vehicles like the ATV (Automated Transfer Vehicle) developed by the European Space Agency[1] and the Orion spacecraft by NASA[2] only rely on the use of jet actuators to perform attitude control.

The bang-bang attitude control problem has received a lot of attention in the past. In particular, the problem has been extensively studied in the case of small-angle maneuvers and single axis-maneuvers. In this context, several approximate control techniques involving the use of PWM (Pulse Width Modulation) and PWPFM (Pulse Width Pulse Frequency Modulation) have been proposed. A review of these techniques can be found in the book by Wie.[3]

Agrawal and Bang[4] have proposed bang-bang controllers for the cases of single-axis, planar maneuvers, while Burdick et al.[5] have proposed a bang-bang controller for the case of small-angle maneuvers.[5] Both these controllers were derived from the classic time-optimal controller for double-integrators (for an overview of such controller see the book by Bryson and Ho[6] and the paper by Rao and Bernstein[7]). These control laws are based on the definition of dead-bands around the parabolic switching curve, which makes the control law robust with respect to uncertainty in the system parameters.

In the past, the problem of time-optimal rest-to-rest reorientation of a rigid body has been extensively studied by the aerospace community. As shown by Bilimoria and Wie[8] for inertially symmetric rigid bodies, if each control torque about each axis of the spacecraft is constrained in a given interval, then the time-optimal solutions are bang-bang. Moreover, the control inputs switch value a total of five times if the reorientation angle is smaller then 72 deg. and a total of seven times otherwise. These features of the time-optimal solutions were only observed in simulation, no rigorous proof was provided. Interestingly, the simulations showed that the eigenaxis maneuver is not the time-optimal maneuver. The controller values and switching times were computed numerically, using continuation techniques whose details were omitted.

Byers and Visali[9] extended this result to asymmetric rigid bodies, under the assumption that the applied torque is significantly larger than the nonlinear gyroscopic terms appearing in the Euler equations. Approximate solutions were derived to compute the controller switching times using numerical procedures. In this context, Bilimoria and Wie's results were confirmed.

*PhD Candidate, Electrical and Computer Engineering Department; edoardo.serpelloni@mail.utoronto.ca.

†Professor, Electrical and Computer Engineering Department; maggiore@control.utoronto.ca.

‡Professor, University of Toronto Institute for Aerospace Studies; damaren@utias.utoronto.ca. Associate Fellow AIAA.

More recently, Bai and Junkins[10] have extended Bilimoria and Wie's numerical work, finding, by using hybrid numerical algorithms, trajectories with six switches for reorientation angles less then 72 deg.

Shen and Tsiotras[11] have studied the problem of time-optimal reorientation of axi-symmetric spacecraft, with nonzero initial angular velocity, by using only two control torques. As above, the optimal solutions were obtained numerically.

The control techniques reviewed above rely on numerical schemes for the computation of the control values and switching times. Initial guesses for the states, controls, co-states etc. are often required.[11] As is to be expected, these controllers are inherently non-robust to external unmodeled perturbations, uncertainty in the system's parameters, or measurement noise.[9]

Krishnan at al.[12] have proposed a solution to the attitude control problem when the spacecraft is actuated along only two axes that does not rely on numerical solutions. The proposed strategy is composed of a sequence of eight separate maneuvers. During the first phase, a discontinuous controller is applied to bring the spacecraft to a rest configuration (zero angular velocity). Once this objective is achieved, several consecutive one axis bang-bang maneuvers are implemented that exploit the structure of the kinematic and dynamic equations. As noted by the authors this controller suffers from a lack of robustness in that it does not offer any stability guarantees. For example, an unmodeled disturbance may prevent the controller from completing one of these phases, therefore breaking down the regulation mechanism.

Sliding mode controllers have been proposed to solve the attitude control problem. Among others, Singh and Iyer have proposed[13] a sliding mode controller for the attitude stabilization of a spinning spacecraft under the effects of bounded disturbance torques. The proposed controller is composed of two parts: a continuous component and a bang-bang component. The controller successfully stabilizes the attitude of the spacecraft under the effects of the external perturbations and explicit expressions for the gains of the switching function are provided. The controller is, however, sensitive to chattering and high frequency switching (the switching frequency is theoretically infinite along the switching curve).

The problem of designing a robust bang-bang controller for the stabilization of a rigid body orientation without inducing high frequency switching of the control value remains open. In this paper, we present a hybrid bang-bang stabilizer that solves the attitude control problem for an inertially symmetric rigid spacecraft. In particular, we show that the proposed controller can stabilize any desired orientation to virtually any level of accuracy, while avoiding high frequency switching behavior. This is shown to work assuming the full nonlinear spacecraft dynamics. The controller presented in the following was inspired by the work of the authors on the practical stabilization of double integrators affected by matched disturbances.[14–16] Simulation results are provided that verify the effectiveness of the proposed controller. The properties of disturbance rejection and robustness are not proved rigorously but they are verified through simulations.

The paper is organized as follows. In Section II we introduce the spacecraft model. We discuss the attitude parametrization used throughout the paper and the actuators used to generate bang-bang torques about each axis. We also present a formal problem statement. In Section III we present a controller for the special case of planar rotations. In Section IV the final controller is presented for general maneuvers. An idea of the proof is presented in the appendix. In Section V we provide some simulation results to show the effectiveness of the proposed controller. We show that the proposed controller meets all the control specifications. In Section VI we introduce possible avenues for future research.

Notation: We denote $B_\epsilon(0) = \{x \in \mathbb{R}^2 : (x^T x)^{1/2} < \epsilon\}$ and $\bar{B}_\epsilon(0) = \{x \in \mathbb{R}^2 : (x^T x)^{1/2} \leq \epsilon\}$. These definitions imply that the set $B_0(0)$ is empty, while $\bar{B}_0(0) = \{0\}$. The 3×3 identity matrix is denoted by $1_{3\times 3}$. Throughout the paper sets are denoted by capital letters. The boundary of a set A is defined as $\partial A = \bar{A} \setminus \mathrm{Int}A$ where $\bar{A}$ is the closure of A and $\mathrm{Int}A$ is its interior.

II. Model and Problem Statement

The spacecraft model developed in this section is standard. We denote by $\mathcal{I} = \{x_\mathcal{I}, y_\mathcal{I}, z_\mathcal{I}\}$ the inertial frame and by $\mathcal{B} = \{x_\mathcal{B}, y_\mathcal{B}, z_\mathcal{B}\}$ the body frame attached to the spacecraft's center of mass and aligned along the principal axes of the spacecraft. Throughout the paper we consider the case of an inertially symmetric spacecraft, i.e. we assume that in frame $\mathcal{B}$ the moment of inertia tensor of the spacecraft is $\bar{J}1_{3\times 3}$, where $\bar{J}$ is the moment of inertia about each principal axis. We assume that the spacecraft is actuated by six clusters of jet thrusters. Each of these clusters is composed by two jet thrusters providing only a constant level of thrust. The torques generated by these actuators are the control inputs of the system, τ_1, τ_2, τ_3 in Figure

1. We assume here that the thrusters are distributed over the surface of the spacecraft so as to generate bang-bang torques independently about each axis, i.e. $\tau_k \in \{-\bar{\tau}_k, 0, +\bar{\tau}_k\}$, with $\bar{\tau}_k > 0$, for $k = 1, 2, 3$.

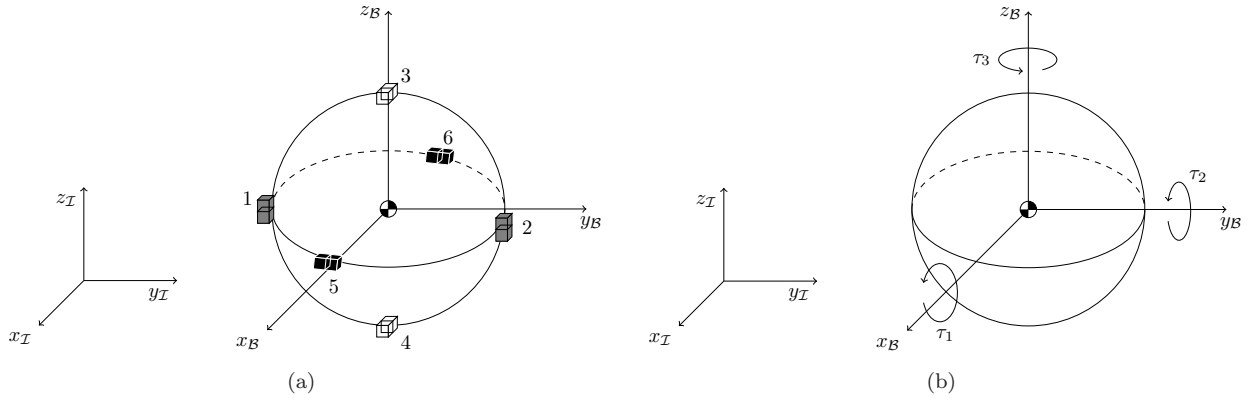

Figure 1. Generation of the control torques.

Throughout the paper we parametrize the attitude of the spacecraft by using the 3-2-1 Euler angles, $\theta = (\theta_1, \theta_2, \theta_3)$, with $-\pi \leq \theta_1, \theta_3 < \pi$ and $-\pi/2 < \theta_2 < \pi/2$. The orientation of the rigid body is then obtained by first rotating frame $\mathcal{I}$ about the third axis by an angle θ_3, then rotating about the new second axis by an angle θ_2 and finally by rotating about the current first axis by an angle θ_1. Let $H = (-\pi, +\pi] \times \left(-\frac{\pi}{2}, +\frac{\pi}{2}\right) \times (-\pi, +\pi]$. The state of the system is $\chi = \mathrm{col}\,(\theta, \omega) \in H \times \mathbb{R}^3$, where

$\theta = \mathrm{col}\,(\theta_1, \theta_2, \theta_3)$: orientation (roll, pitch and yaw angles).

$\omega = \mathrm{col}\,(\omega_1, \omega_2, \omega_3)$: angular velocity in frame $\mathcal{B}$.

Let $u = \bar{J}^{-1}\tau = (u_1, u_2, u_3)$. Then $u_k \in U_k = \{-\bar{u}_k, 0, +\bar{u}_k\}$, with $\bar{u}_k = \bar{\tau}_k/\bar{J} > 0$, for $k = 1, 2, 3$. The spacecraft rotational dynamics can therefore be modeled as follows:

$$\begin{aligned} \dot{\theta} &= \begin{bmatrix} 1 & \sin\theta_1 \tan\theta_2 & \cos\theta_1 \tan\theta_2 \\ 0 & \cos\theta_1 & -\sin\theta_1 \\ 0 & \sin\theta_1 \sec\theta_2 & \cos\theta_1 \sec\theta_2 \end{bmatrix} \omega \\ \dot{\omega} &= u. \end{aligned} \tag{1}$$

In this paper we propose a solution to the following problem.

Attitude Control Problem (ACP): Consider system (1) modeling the rotational dynamics of a symmetric spacecraft. Design a bang-bang feedback controller $u = (u_1, u_2, u_3)$, $u_k \in \{-\bar{u}_k, 0, +\bar{u}_k\}$, such that

i) the origin is made practically stable for the closed-loop system. In other words, there exists a neighborhood of the origin in $H \times \mathbb{R}^3$, containing the origin in its interior, such that for any initial condition $\chi(0)$ chosen in such neighborhood and for any open set V, with $0 \in \mathrm{Int}V$, there exist controller parameters and there exists $T \geq 0$ such that for all $t \geq T$, $\chi(t) \in V$.

ii) Each thruster fires a finite number of times over any compact time interval.

III. Special Case: Single-Axis Maneuver

We begin our exploration of the attitude control problem with the special case of planar rotations about one of the body axes. Thus we consider the model of a single-axis rotation:

$$\begin{aligned} \dot{\theta} &= \omega \\ \dot{\omega} &= u. \end{aligned} \tag{2}$$

The objective is to practically stabilize $(\theta, \omega) = (0, 0)$. The problem, therefore, is reduced in this context to the stabilization of a double-integrator with bang-bang control. The challenge of this double-integrator stabilization problem is the requirement that the controller should be bang-bang and, at the same time, it should not induce high-frequency switching of the control value. The problem was recently solved by Serpelloni et al.[14–16] We now briefly review the solution.

Let $\chi = (\theta, \omega) \in (-\pi, +\pi] \times \mathbb{R}$ denote the state of system (2) and let $u \in \{-\bar{u}, 0 + \bar{u}\}$ be the control input. Referring to Figures 2(a) and 2(b), define **initialization sets** Γ^+, Γ^- as

$$\begin{aligned} \Gamma^+ =& \{(\theta, \omega) : \theta < 0,\ \omega < \sqrt{-2\bar{u}\theta}\} \cup \{(\theta, \omega) : \theta > 0,\ \omega \leq -\sqrt{2\bar{u}\theta}\}, \\ \Gamma^- =& \{(\theta, \omega) : \theta < 0,\ \omega \geq \sqrt{-2\bar{u}\theta}\} \cup \{(\theta, \omega) : \theta > 0,\ \omega > -\sqrt{2\bar{u}\theta}\}. \end{aligned} \tag{3}$$

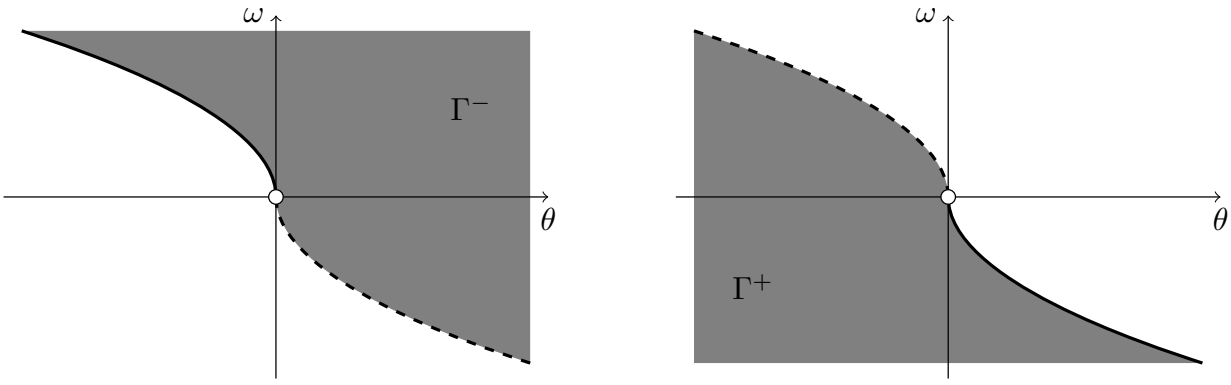

(a) Initialization set Γ^-.

(b) Initialization set Γ^+.

Figure 2.

Referring to Figure 3, define **switching sets** Λ^+, Λ^- as

$$\begin{aligned} \Lambda^+ =& \{(\theta, \omega) : \theta \leq 0,\ \omega \leq 0\} \cup \{(\theta, \omega) : \theta > 0,\ \omega \leq -\sqrt{2\bar{u}\theta}\}, \\ \Lambda^- =& \{(\theta, \omega) : \theta \geq 0,\ \omega \geq 0\} \cup \{(\theta, \omega) : \theta < 0,\ \omega \geq \sqrt{-2\bar{u}\theta}\}. \end{aligned} \tag{4}$$

The boundaries of sets Λ^+ and Λ^- are given by

$$\partial\Lambda^+ = S^+ \cup \{(\theta, 0) : \theta \leq 0\} \quad \partial\Lambda^- = S^- \cup \{(\theta, 0) : \theta \geq 0\}, \tag{5}$$

where S^+, S^- are half-parabolas

$$S^+ = \{(\theta, -\sqrt{2\bar{u}\theta}) : \theta > 0\} \quad S^- = \{(\theta, \sqrt{-2\bar{u}\theta}) : \theta < 0\}.$$

The proposed control law is described by the automaton $\mathcal{A}_\theta$ in (7), and is characterized by discrete states $Q = \{q_1, q_2, q_3\}$ and continuous states χ. The controller satisfies property (ii) of ACP thanks to the implementation of an hysteresis mechanism at the origin based on the definition of two nested balls of radius $0 < \delta_1 < \delta_2$. The control value is given by the hybrid feedback $u^\star : Q \to \mathbb{R}$ defined as

$$\begin{aligned} u^\star(q_1) &= -\bar{u} \\ u^\star(q_2) &= +\bar{u} \\ u^\star(q_3) &= 0. \end{aligned} \tag{6}$$

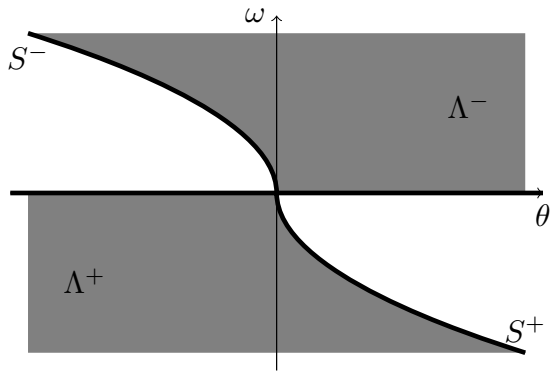

Figure 3. The switching sets Λ^-, Λ^+.

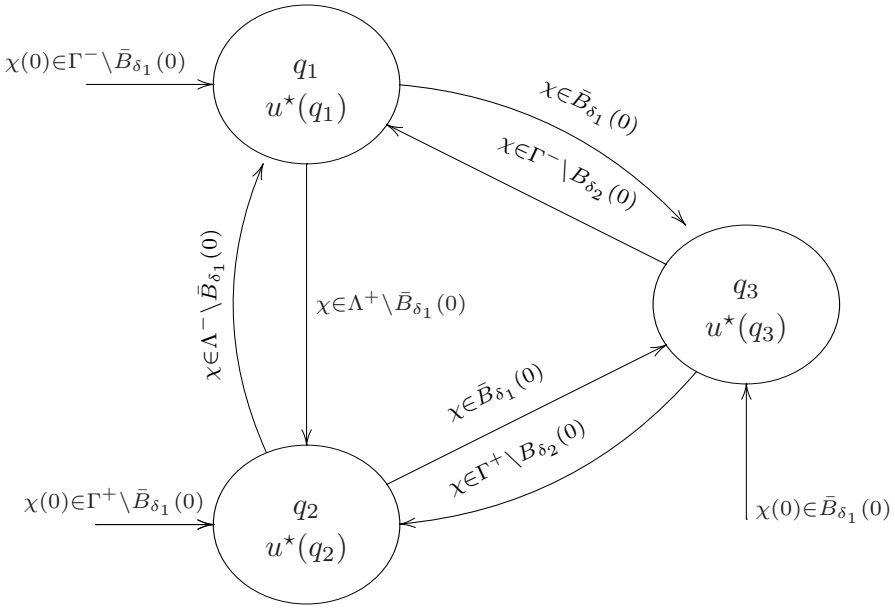

(7)

We have shown in previous papers[14–16] that controller (6)-(7), by a suitable choice of parameters, globally practically stabilizes any neighborhood of the origin for a double-integrator system. Moreover, we have shown that the controller is insensitive to matched disturbances (i.e. disturbances appearing in the second channel of the double-integrator system), measurement noise and actuator uncertainties. In the case of a rotational double-integrator as in (2) these results hold only locally, in that it must be guaranteed that $\theta \in (-\pi, +\pi)$.

IV. Generalization: Solution of ACP

In the previous section we have presented a bang-bang controller for planar, single-axis maneuvers. Now we simply apply three copies of such controller about the three principal axes of the spacecraft. Remarkably, this decentralized control strategy works despite the coupled nature of the attitude dynamics. Model (1) can be rewritten as a collection of three coupled double integrators with nonlinear coupling terms:

$$\begin{aligned}
\dot{\theta}_1 &= \omega_1 + \omega_2 \sin\theta_1 \tan\theta_2 + \omega_3 \cos\theta_1 \tan\theta_2 \\
\dot{\omega}_1 &= u_1 \\
\dot{\theta}_2 &= \omega_2 \cos\theta_1 - \omega_3 \sin\theta_1 \\
\dot{\omega}_2 &= u_2 \\
\dot{\theta}_3 &= \omega_3 \cos\theta_1 \sec\theta_2 + \omega_2 \sin\theta_1 \sec\theta_2 \\
\dot{\omega}_3 &= u_3.
\end{aligned} \tag{8}$$

Let $\chi_1 = (\theta_1, \omega_1) \in (-\pi, +\pi] \times \mathbb{R}$, $\chi_2 = (\theta_2, \omega_2) \in (-\pi/2, +\pi/2) \times \mathbb{R}$, $\chi_3 = (\theta_3, \omega_3) \in (-\pi, +\pi] \times \mathbb{R}$ denote the state of each subsystem in (8). Our approach considers the nonlinearities in (8) as unknown vanishing perturbations disturbing the dynamics of the system. Indeed, if we define the following functions $H \times \mathbb{R}^3 \to \mathbb{R}$

$$\begin{aligned} c_1(\chi) &= 1 \\ f_1(\chi) &= \omega_2 \sin\theta_1 \tan\theta_2 + \omega_3 \cos\theta_1 \tan\theta_2 \\ c_2(\chi) &= \cos\theta_1 \\ f_2(\chi) &= -\omega_3 \sin\theta_1 \\ c_3(\chi) &= \cos\theta_1 \sec\theta_2 \\ f_3(\chi) &= \omega_2 \sin\theta_1 \sec\theta_2, \end{aligned} \tag{9}$$

then systems (8) can be rewritten as follows

$$\begin{aligned} \dot{\theta}_1 &= c_1(\chi)\omega_1 + f_1(\chi) \\ \dot{\omega}_1 &= u_1 \end{aligned} \tag{10}$$

$$\begin{aligned} \dot{\theta}_2 &= c_2(\chi)\omega_2 + f_2(\chi) \\ \dot{\omega}_2 &= u_2 \end{aligned} \tag{11}$$

$$\begin{aligned} \dot{\theta}_3 &= c_3(\chi)\omega_3 + f_3(\chi) \\ \dot{\omega}_3 &= u_3, \end{aligned} \tag{12}$$

where $c_k, f_k \to 0$ as $\chi \to 0$, with $k = 1, 2, 3$. Each of these subsystems can be interpreted as a rotational double integrator with state χ_k perturbed in the first channel by vanishing perturbations c_k and f_k.

We propose to solve ACP by applying controller (6)-(7) to each subsystem (10) to (12). This strategy corresponds to performing control of the spacecraft rotational dynamics by actuating each axis independently (see Figure 4 for a pictorial representation). Let then each control input u_k be given by $u_k^\star : \mathcal{Q}_k \to \mathbb{R}$, with $k = 1, 2, 3$, where $q^k \in \mathcal{Q}_k = \{q_1^k, q_2^k, q_3^k\}$

$$\begin{aligned} u_k^\star(q_1) &= -\bar{u}_k \\ u_k^\star(q_2) &= +\bar{u}_k \\ u_k^\star(q_3) &= 0. \end{aligned} \tag{13}$$

The evolution of the discrete state q^k is driven by the associated automaton $\mathcal{A}_{\theta_k}$. Each automaton $\mathcal{A}_{\theta_k}$, induces state transitions only based on state χ_k of the associated subsystem. The final controller is therefore given by

$$u = \begin{pmatrix} u_1^\star(q^1) \\ u_2^\star(q^2) \\ u_3^\star(q^3) \end{pmatrix} \tag{14}$$

with automata $\mathcal{A}_{\theta_1}, \mathcal{A}_{\theta_2}, \mathcal{A}_{\theta_3}$.
Referring to the spacecraft model (1), each automaton will then coordinate the on-off switches of the thrusters belonging to the two clusters actuating the same axis of the spacecraft.

Theorem 1. Consider system (1) with hybrid feedback controller (14), driven by automata $\mathcal{A}_{\theta_k}$, $k = 1, 2, 3$, as in Figure 4. If $\bar{u}_k$, with $k = 1, 2, 3$, is chosen sufficiently large, then controller (14) solves ACP.

An idea of the proof is presented in the appendix.

V. Simulations

In this section we present some simulation results in order to prove the effectiveness of controller (14) in stabilizing the orientation of a spinning spacecraft. Below are listed the main parameters used in the simulation. For simplicity we modeled the vehicle as a sphere with uniformly distributed mass.

Diameter of the vehicle: $D = 4.5$ m.

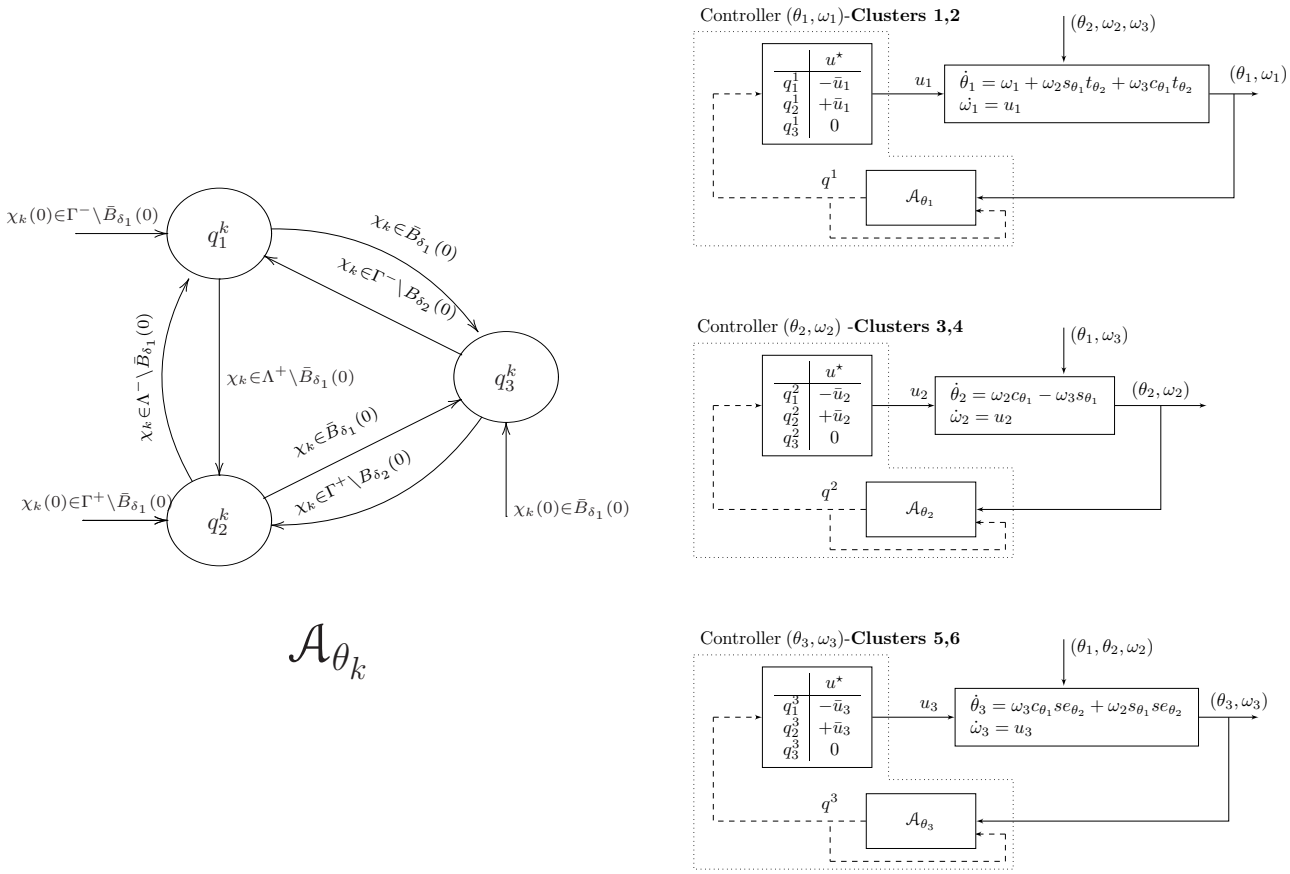

Figure 4. Block diagram representing system (1) with hybrid feedback controller (14) with automata $\mathcal{A}_{\theta_k}$. Discrete state signals are represented using a dotted line, while continuous states are represented using a solid line. Notice that while the dynamics of the plant are fully coupled, the torque applied about each axis of the spacecraft depends only on the state of the associated subsystem. Each axis of the spacecraft is therefore actuated independently.

Mass of the vehicle: $20,750$ kg.

Moment of Inertia about the principal axes: $\bar J = 4.2019 \cdot 10^4$ kg $\cdot$ m^2.

Thrust delivered by each thrusters: 200 N.

Parameter: $\bar u_k$, $\bar u_k = 0.021$ rad/s^2.

The data used in the simulations are inspired by the characteristics of the ATV (Automated Transfer Vehicle) developed by ESA.[1,17,18] ATV supplies the ISS with food, fuel and scientific equipment. The vehicle is completely automated and performs multiple rendezvous and docking operations that involve large attitude maneuvers. This case represents an ideal benchmark for the proposed control strategy. We consider the following initial conditions:

$$\theta(0) = (-7\pi/15, -\pi/3, 2\pi/3) \quad \omega(0) = (-0.05, 0.02, 0.02)\,\text{rad/s}.$$

The selected initial conditions are representative of the typical spinning rates of space vehicles just released from the launcher.

A. Nominal System

The simulation is stopped when the state trajectory of all three subsystems enters a neighborhood of the origin of radius $5 \cdot 10^{-6}$. Figures 5(a) to 7(b) show the state trajectory for the three coupled subsystems (10) to (12) with the proposed controller. Figures 5(a) to 7(a) show that $\chi_1(t), \chi_2(t), \chi_3(t)$ converge to the

origin. Figures 5(b) to 7(b) show a zoom of the state trajectory in a small neighborhood of the origin. The controller stabilizes the desired vehicle orientation. Figures 8(a) to 8(b) show the time history of the Euler angles and the three angular velocities during the simulation. All these figures clearly show that the controller successfully stabilizes the desired attitude. Figure 9 provides a pictorial representation of the rotation undergone by the vehicle when the proposed controller is applied. The figure shows the initial and final orientation of the body frame seen from the inertial frame $\mathcal{I}$. Figure 10 shows the time history of the applied torque. In the figure we show the variable $\sigma_k = u_k/\bar{u}_k$, with $k = 1, 2, 3$, i.e. the normalization of the applied torque. As claimed above the controller fires the thrusters a finite number of times; in fact it takes a finite number of on-off cycles to enter a neighborhood of the origin of radius $5 \cdot 10^{-6}$.

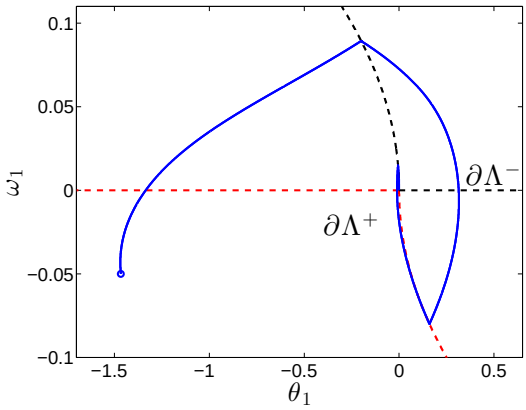

(a) State trajectory of the (θ_1, ω_1)-subsystem.

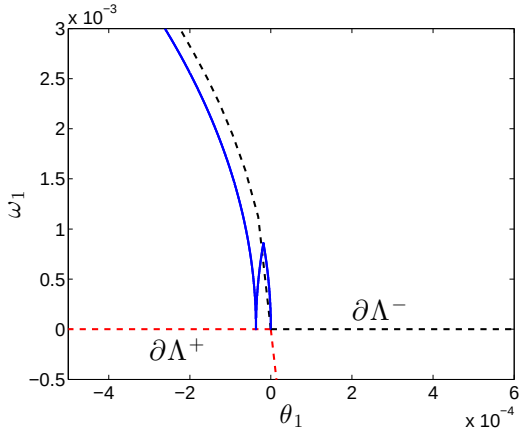

(b) Zoom of the state trajectories in a neighborhood of the origin of the (θ_1, ω_1)-subsystem.

Figure 5.

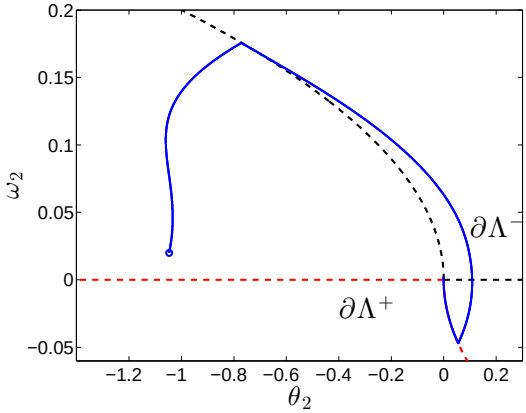

(a) State trajectory of the (θ_2, ω_2)-subsystem.

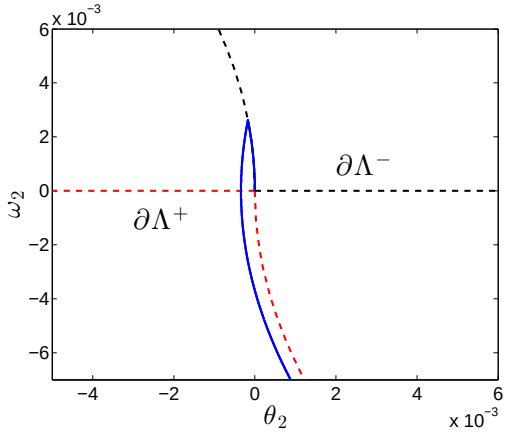

(b) Zoom of the state trajectories in a neighborhood of the origin of the (θ_2, ω_2)-subsystem.

Figure 6.

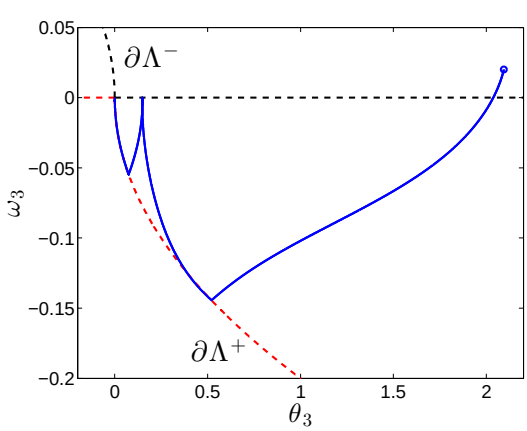

(a) State trajectory of the (θ_3, ω_3)-subsystem.

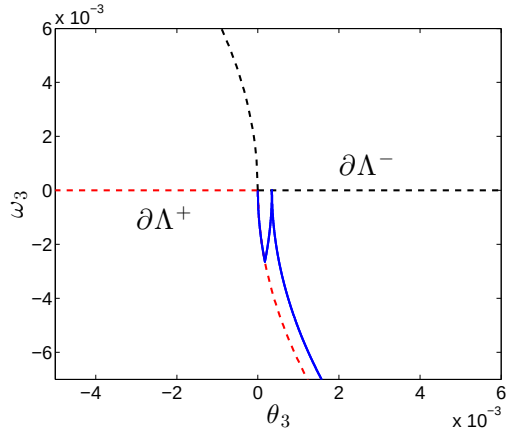

(b) Zoom of the state trajectories in a neighborhood of the origin of the (θ_3, ω_3)-subsystem.

Figure 7.

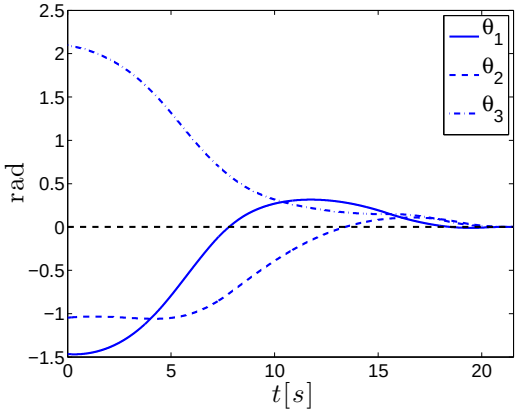

(a) Time history of Euler angles $(\theta_1, \theta_2, \theta_3)$.

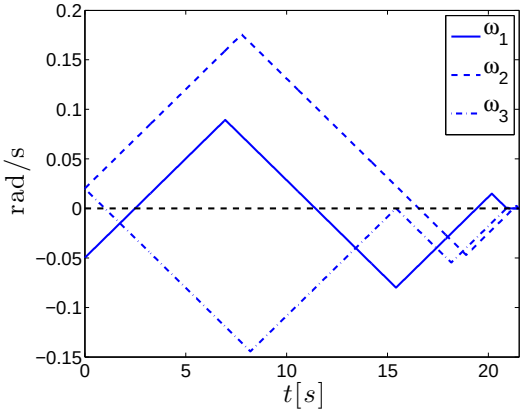

(b) Time history of the angular velocities $(\omega_1, \omega_2, \omega_3)$.

Figure 8.

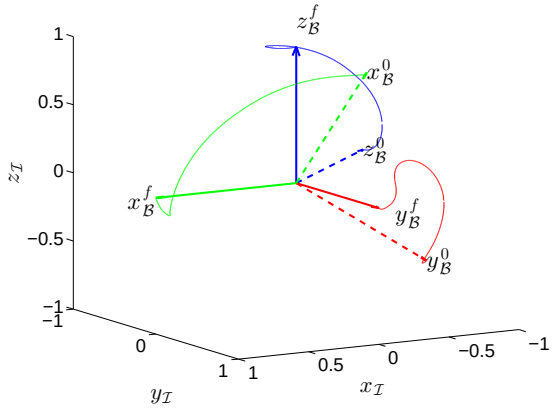

Figure 9. Rotation performed by the vehicle during the simulation. Initial orientation of the vehicle, i.e. frame $\{x_{\mathcal{B}}^0, y_{\mathcal{B}}^0, z_{\mathcal{B}}^0\}$ is represented by dotted lines, while the final orientation, i.e. frame $\{x_{\mathcal{B}}^f, y_{\mathcal{B}}^f, z_{\mathcal{B}}^f\}$ is represented using solid lines ($x_{\mathcal{B}}$ in green, $y_{\mathcal{B}}$ in red, $z_{\mathcal{B}}$ in blue).

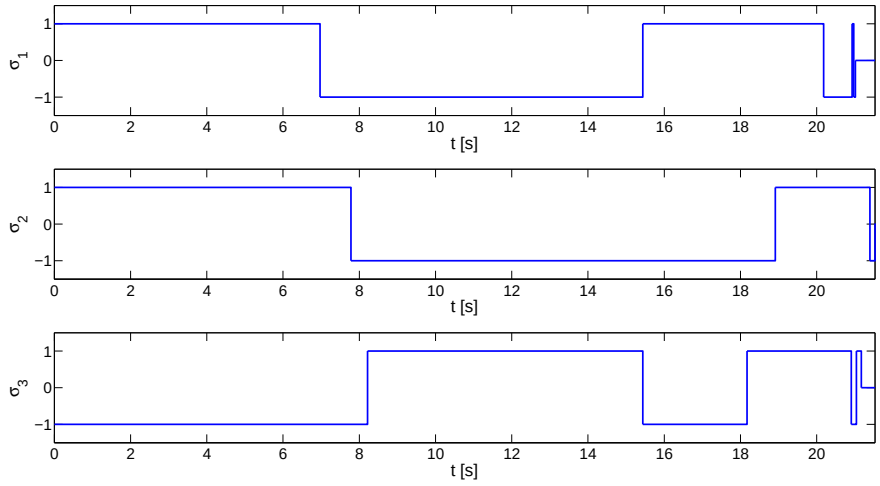

Figure 10. Normalized torque applied about the spacecraft axis.

B. Robustness with Respect to External Perturbations

In this section we test the robustness of the proposed controller with respect to external perturbations. A theoretical analysis of the robustness with respect to external torques will be the subject of future research. In this context we limit ourselves to showing a few simulation results verifying that the proposed controller can successfully reject a small external perturbation. We consider the following perturbation

$$\tau_e = \begin{pmatrix} d_1 \sin t \\ d_2 \sin 0.1t \\ d_3 \cos 0.5t \end{pmatrix},$$

where $d_1 = 8.4038\ \mathrm{N \cdot m}$, $d_2 = 12.6057\ \mathrm{N \cdot m}$ and $d_3 = -16.8076\ \mathrm{N \cdot m}$. We want to show that the proposed controller can keep the state in any arbitrarily small neighborhood of the origin. Notice that open balls $B_{r_k}(0)$ can, without any loss of generality be substituted by open boxes $U_k = (-\delta\theta_k, +\delta\theta_k) \times (-\delta\omega_k, +\delta\omega_k)$ where $\delta\theta_k$ and $\delta\omega_k$ are the desired tolerances on each Euler angle and angular velocity that the designer wants to enforce. In this simulation we enforce the following tolerances:

$$\delta\theta_k = 4 \cdot 10^{-5}\ \mathrm{rad}, \quad \delta\omega_k = 1 \cdot 10^{-3}\ \mathrm{rad/s}.$$

Figures 11(a), 12(a) and 13(a) show that, despite the external disturbances, the state trajectory is driven to the desired neighborhood of the target configuration. Figures 11(b), 12(b) and 13(b) confirm that, via a proper choice of the control parameters, the state trajectory of each subsystem never leaves the desired neighborhood U_k, $k = 1, 2, 3$. This allows us to enforce the desired level of tolerance despite the presence of external torques perturbing the system's dynamics. Euler angles and angular velocities during the simulation are shown in Figures 14(a) and 14(b). Notice, from Figures 15(a) to 17(b) , how for each subsystem the proposed controller meets the control specifications despite the presence of external disturbances. The normalized torques applied to each axis of the spacecraft are shown Figure 18. The figure clearly illustrates how the controller achieves the control objective without inducing high-frequency switching.

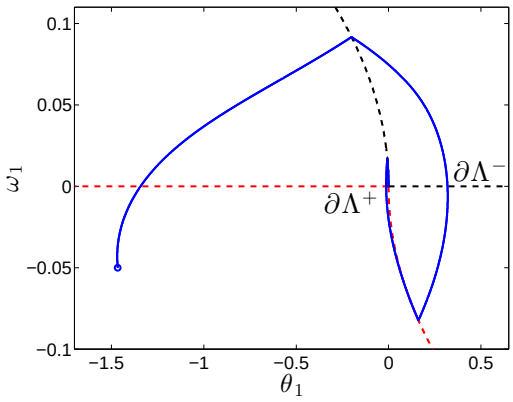

(a) State trajectory of the (θ_1, ω_1)-subsystem.

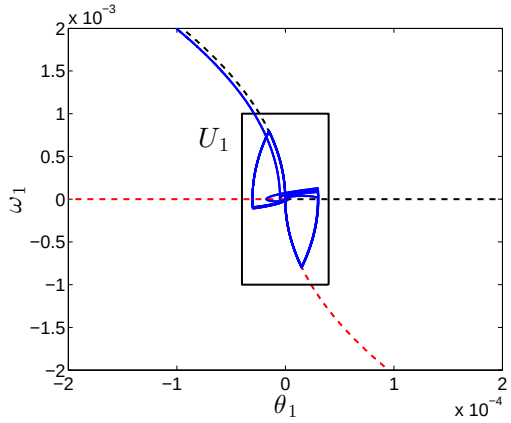

(b) State trajectory of the (θ_1, ω_2)-subsystem in a neighborhood of the origin. The state remains in U_1.

Figure 11.

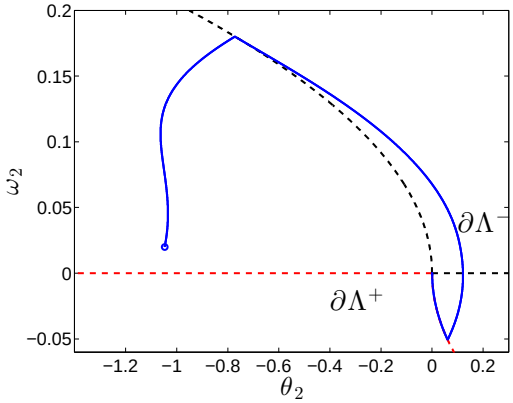

(a) State trajectory of the (θ_2, ω_2)-subsystem.

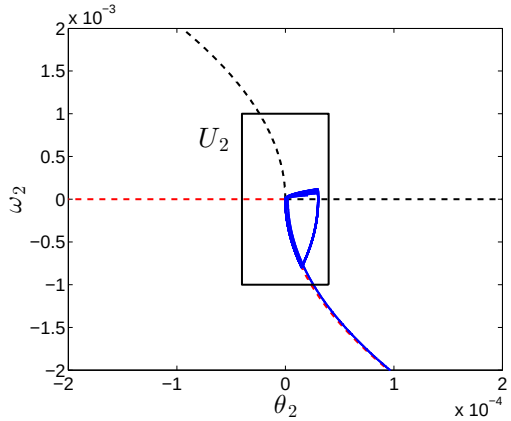

(b) State trajectory of the (θ_2, ω_2)-subsystem in a neighborhood of the origin. The state remains in U_2.

Figure 12.

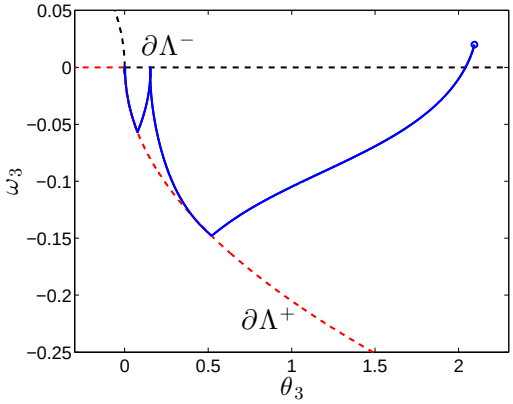

(a) State trajectory of the (θ_1, ω_1)-subsystem.

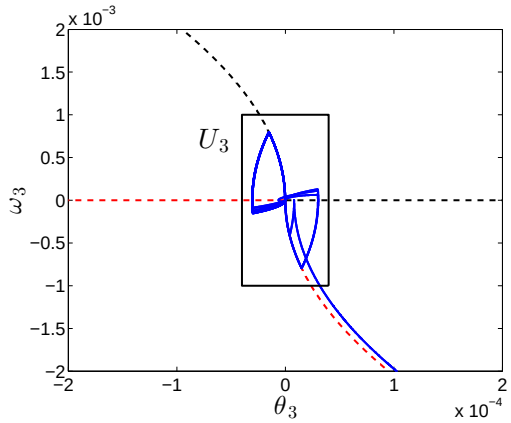

(b) State trajectory of the (θ_3, ω_3)-subsystem in a neighborhood of the origin. TThe state remains in U_3.

Figure 13.

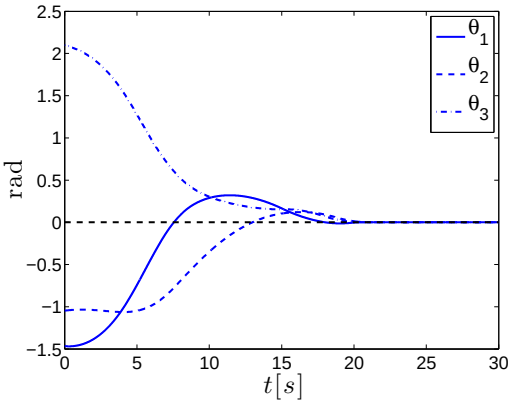

(a) Time history of the Euler angles $(\theta_1, \theta_2, \theta_3)$.

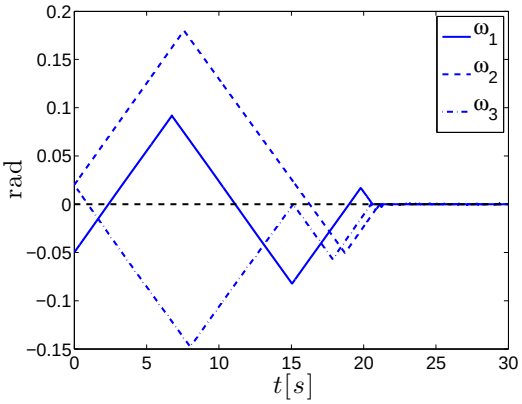

(b) Time history of the angular velocities $(\omega_1, \omega_2, \omega_3)$.

Figure 14.

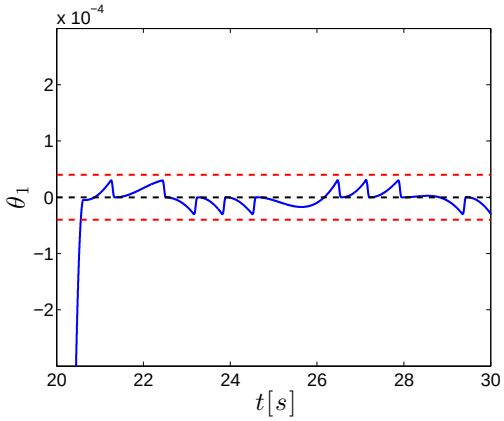

(a) θ_1 is successfully kept in the prescribed bounds.

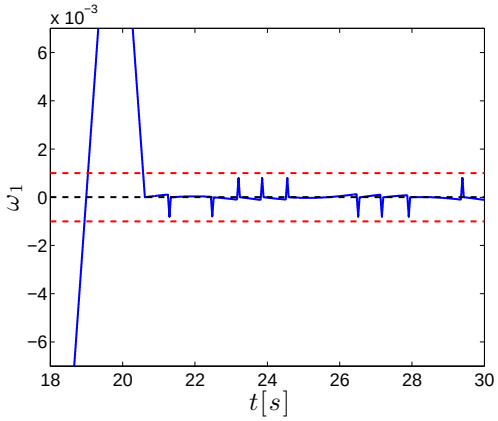

(b) ω_1 is successfully kept in the prescribed bounds.

Figure 15.

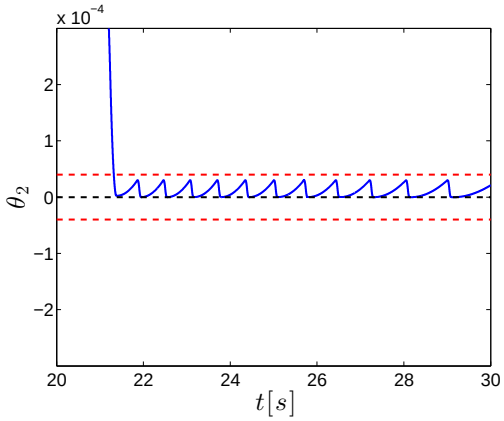

(a) θ_2 is successfully kept in the prescribed bounds.

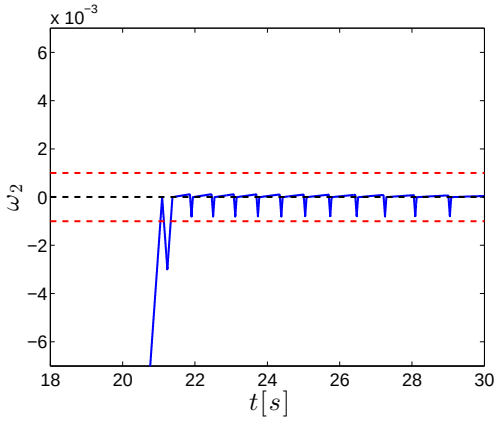

(b) ω_2 is successfully kept in the prescribed bounds.

Figure 16.

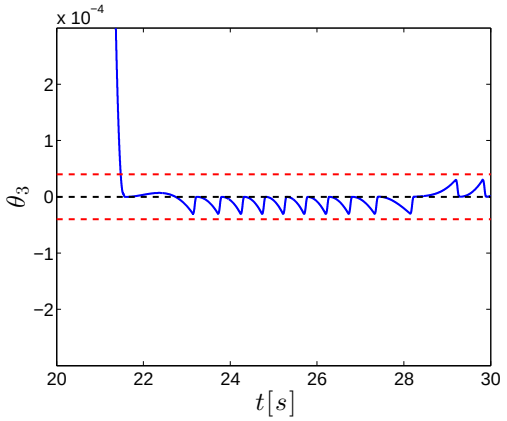

(a) θ_3 is successfully kept in the prescribed bounds.

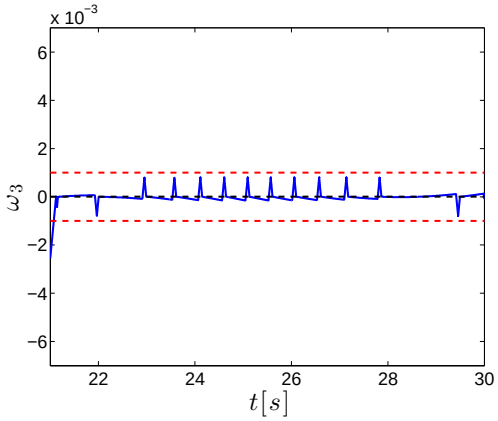

(b) ω_3 is successfully kept in the prescribed bounds.

Figure 17.

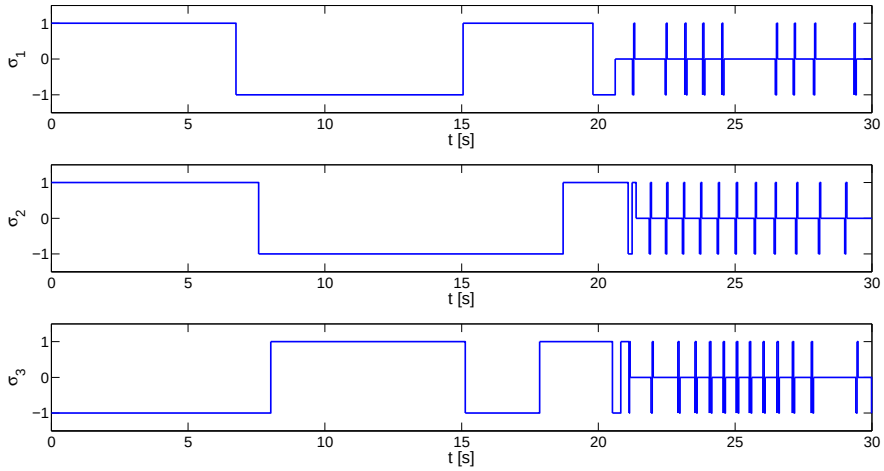

Figure 18. Normalized torque applied about each axis of the spacecraft.

VI. Conclusions

In the paper we presented a novel hybrid bang-bang controller that solves the attitude control problem. We have proved that this controller successfully stabilizes a target configuration to any degree of accuracy without high-frequency switchings of the actuators. The full nonlinear rotational dynamics of the spacecraft is considered in the analysis of the controller's performances. Moreover, we have shown in simulation that the controller is robust with respect to small external perturbations.

Appendix: Idea of the Proof

In this section we present a sketch of the proof of Theorem 1. For the sake of clarity we consider the case of only two control torques, about spacecraft axes $x_{\mathcal{B}}$ and $y_{\mathcal{B}}$ and we show that $z_{\mathcal{B}}$ is stabilized to a target neighborhood of a desired orientation in frame $\mathcal{I}$. The complete, formal proof of Theorem 1 is lengthy and beyond the scope of this paper. It will be presented elsewhere.

In this section we therefore consider the following system

$$\begin{aligned}\dot{\theta}_1 &= c_1(\chi)\omega_1 + f_1(\chi)\\ \dot{\omega}_1 &= u_1\\ \dot{\theta}_2 &= c_2(\chi)\omega_2 + f_2(\chi)\\ \dot{\omega}_2 &= u_2,\end{aligned} \tag{15}$$

where each control input u_k is given by hybrid controller (13), with $k = 1, 2$. As before, the state of each subsystem of (15) is denoted by $\chi_k = (\theta_k, \omega_k)$, $k = 1, 2$. Notice that for any initial condition $(\theta_3(0), \omega_3(0))$, $\omega_3(t) = \omega_3(0) = \bar{\omega}_3$. Moreover, system (15) does not depend on θ_3. A solution of (15) though an initial condition $(\chi_1(0), \chi_2(0))$ is denoted by $(\chi_1(t), \chi_2(t))$. We show that for any $r > 0$ there exists controller parameters and there exists $T > 0$ such that for all $t \geq T$, $(\chi_1(t), \chi_2(t)) \in B_r(0) \times B_r(0)$.
We start by defining the concepts of *switching point* and *switching time*.

Definition 1. Let $(\chi_1(t), \chi_2(t))$ be a solution of system (15) with control inputs u_k given by hybrid feedback (6)-(7), $k = 1, 2$. A time instant t_i, with $i \in \mathbb{N}$, is called a **switching time** for χ_k, with $k = 1, 2$, if $\chi_k(t_i) \in \left(S^+ \cup S^- \cup \bar{B}_{\delta_1}(0)\right)$ and at time $t = t_i$ a state transition $q_j^k \to q_m^k$, with $j, m \in \{1, 2, 3\}$, $j \neq m$ occurs. The value of the state at a switching time, $\chi_k^i = \chi_k(t_i)$ is called a **switching point**. △

The proof of Theorem 1 unfolds in three main steps.

Step 1: Solutions bundles and positive invariant sets

Let $\bar{\theta}_1, \bar{\theta}_2 < \frac{\pi}{2}$. In this step of the proof we show that there exists a positively invariant set $\Theta_1 \times \Theta_2$ for system (15) with controllers as in (13).To start let $\delta_1 = \delta_2 = 0$.

a) Solutions bundle for the (θ_2, ω_2)-subsystem
Consider the (θ_2, ω_2)-subsystem and suppose that angle θ_1 remains bounded by $\pm\bar{\theta}_1$, i.e. $|\theta_1(t)| \leq \bar{\theta}_1$. Hence, since θ_1 and ω_3 are bounded, functions c_2 and f_2 remain bounded in $[\bar{c}_2, +1]$ and $\left[-\bar{f}_2, +\bar{f}_2\right]$, with $\bar{c}_2 = \cos\bar{\theta}_1$ and $\bar{f}_2 = \bar{\omega}_3 \sin\bar{\theta}_1$, respectively. Then, without any loss of generality, c_2 and f_2 can be seen as piecewise continuous time-varying exogenous signals $c_2(t) \in [\bar{c}_2, +1]$, $f_2(t) \in \left[-\bar{f}_2, +\bar{f}_2\right]$. The (θ_2, ω_2)-subsystem can therefore be rewritten as follows

$$\begin{aligned}\dot{\theta}_2 &= c_2(t)\omega_2 + f_2(t)\\ \dot{\omega}_2 &= u_2\end{aligned} \tag{16}$$

We need to study the solutions of (16) as c_2 and f_2 vary among **all** the possible piecewise continuous functions bounded by $[\bar{c}_2, +1]$ and $\left[-\bar{f}_2, +\bar{f}_2\right]$, respectively. To do so we characterize the solutions bundle of subsystem (16) from any initial condition by applying the theory developed by Maggiore et al.[19] Given any initial condition $\chi_2(0)$, with $|\theta_2(0)| < \bar{\theta}_2$ consider the collection of solutions obtained by varying $c_2(t)$ and $f_2(t)$ and restricting the time interval between $t = 0$ and the time of the first switch of the controller (possibly infinite). One can show that this collection of solutions is the closed set delimited by two **extremal curves** through $\chi_2(0)$, denoted by ϕ_L and ϕ_R, as shown in Figure 19. This set is said to be the **solutions bundle** through $\chi_2(0)$, and we denote it by $B^2(\chi_2(0))$. For any initial condition in $B^2(\chi_2(0))$, the state trajectory will remain in $B^2(\chi_2(0))$ until the trajectory hits the active switching set.

b) Existence of a state transition for (θ_2, ω_2)-subsystem
Consider subsystem (16) with controller (13). As shown in Figure 19 the solutions bundle $B^2(\chi_2(0))$ intersects the next switching set, say Λ^-, if and only if both the extremal curves themselves intersect transversally Λ^-. Since the two extremal curves can be determined analytically, one can easily show that that's the case if and only if $\bar{u}_2 > 0$. This implies that all solutions through an arbitrary initial condition must perform a state transition in finite time. As shown in Figure 19, the state trajectory either hits Λ^- on S^- or on the θ_2-axis. If the trajectory hits Λ^- on the θ_2-axis one can show that the state trajectory must later hit the active switching set Λ^+ on S^+. In either case the state trajectory is forced to return and induce a state transition on either S^+ or S^-. This implies that the proposed controller induces a sequence of switching points $\{\chi_2^i\}$.

c) Positively invariant set for (θ_2, ω_2)-subsystem
Consider $\bar{\chi}_2 = \left(\bar{\theta}_2, \bar{\omega}_2\right) \in S^+$ and consider the solutions bundle from $\bar{\chi}_2$, $B^2(\bar{\chi}_2)$. As explained above the

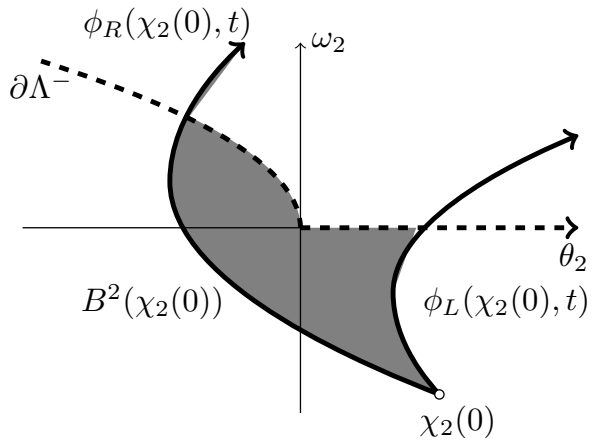

Figure 19. Attainable set of subsystem (16) from $\chi_2(0)$.

state trajectory either switches on S^- or on the θ_2-axis. By constructing the solutions bundle from the possible attainable points on θ_2-axis, one can show that between consecutive switching points the state trajectory will remain inside set $A^2(\bar{\chi}_2)$ (shaded region in Figure 20(a)).
The same set can be built from $-\bar{\chi}_2$. Let $\Theta_2 = A^2(\bar{\chi}_2) \cap A^2(-\bar{\chi}_2)$, as in Figure 20(b).
One can show that if $\bar{u}_2$ is chosen sufficiently large, then Θ_2 is positively invariant. So, as long as $|\theta_1(t)| \leq \bar{\theta}_1$, if $\chi_2(0) \in \Theta_2$, then $\chi_2(t) \in \Theta_2$, for all $t \geq 0$ and $\chi_2^i \in \Theta_2$ for all i. Moreover, if $\bar{u}_2$ is large enough one can also prove that $\Theta_2 \subset \left[-\bar{\theta}_2, +\bar{\theta}_2\right] \times \mathbb{R}$.

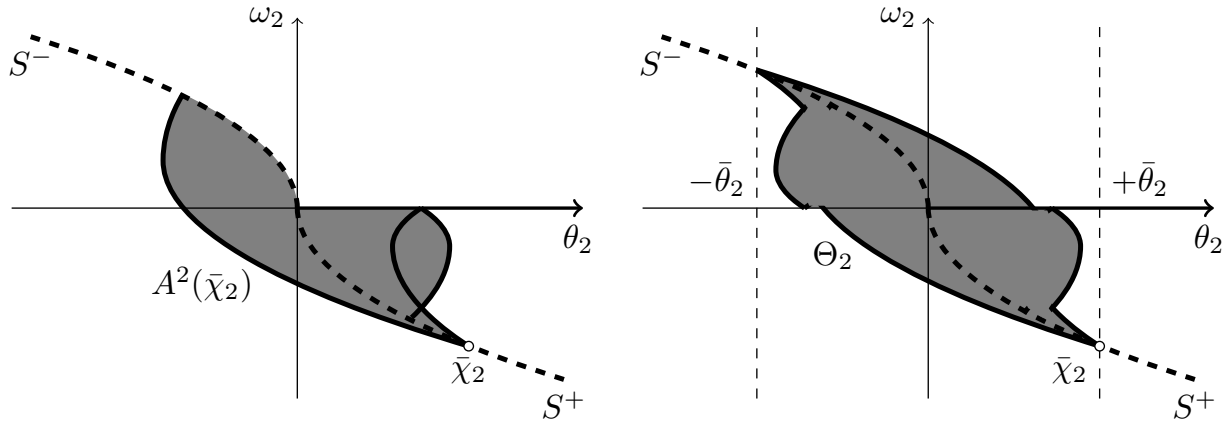

(a) Attainable set of subsystem (16) from $\bar{\chi}_2$ between consecutive switching points.

(b) Positively invariant set Θ_2.

Figure 20.

d) (θ_1, ω_1)-subsystem
Suppose now that $\chi_2(t) \in \Theta_2$. The same procedure described above in points a) to d) can be applied to (θ_1, ω_1)-subsystem. Therefore, we can construct a positively invariant set Θ_1 for the (θ_1, ω_1)-subsystem as well. As above, if $\bar{u}_1$ is chosen large enough one can show that $\Theta_1 \subset \left[-\bar{\theta}_1, +\bar{\theta}_1\right] \times \mathbb{R}$. As in point b)-c) if $\chi_1(0) \in \Theta_2$, then there exists a sequence of switching points $\{\chi_1^i\}$ with $\chi_1^i \in \Theta_1$.

e) Positively invariant set for system (15)
The results presented above only prove the existence of positively invariant sets for **each** subsystem, provided the states of **the other** subsystems remain bounded. It can be easily shown that the product of the two sets $\Theta_1 \times \Theta_2$ is in fact a positively invariant set for system (15). This means that for any $(\chi_1(0), \chi_2(0)) \in \Theta_1 \times \Theta_2$,

$(\chi_1(t), \chi_2(t)) \in \Theta_1 \times \Theta_2,\ \forall t \geq 0.$

Step 2: Extremal switching sequences
So far we have just shown that if we pick the initial conditions in a certain neighborhood of the origin then the trajectory of the state will remain inside such neighborhood. We now need to characterize the sequences of switching points induced by the controllers in order to show that the state trajectory converges to the origin. By studying the properties of the attainable sets of the two subsystems between consecutive switching points, one can define two sequences $\{z_1^i\}$ and $\{z_2^i\}$ such that for any i, $\|\chi_1^i\| \leq \|z_1^i\|$ and $\|\chi_2^i\| \leq \|z_2^i\|$.

Step 3: Convergence
To show convergence of the whole trajectory to the origin we show that the two sequences of switching points $\{\chi_1^i\}$, $\{\chi_2^i\}$ converge to the origin.
By studying the two sequences $\{z_1^i\}$ and $\{z_2^i\}$ one can show that there exists a sequence of positively invariant sets $\{\Theta_1^i \times \Theta_2^i\}$ such that for any i, the state trajectory $(\chi_1(t), \chi_2(t))$ enters in finite time in set $\Theta_1^i \times \Theta_2^i$ and never leaves. It can be shown that set $\Theta_1^i \times \Theta_2^i$ contracts to a single point, the origin, as $i \to \infty$. Therefore, for any $r > 0$, there exists $N > 0$ such that for all $i \geq N$, $\Theta_1^i \times \Theta_2^i \subset B_r(0) \times B_r(0)$. Let then $0 < \delta_2 < r$ so that $\bar{B}_{\delta_2}(0) \subset \Theta_1^N$ and $\bar{B}_{\delta_2}(0) \subset \Theta_2^N$. If one picks $\delta_1 < \delta_2$, the trajectory never leaves $B_r(0) \times B_r(0)$.

Remark 1. The proof of Theorem 1 is very conservative. In particular, the values of $\bar{u}_k$ required to define positively invariant sets Θ_1 and Θ_2 can be prohibitively high when compared with the performances that can be obtained with today's thrusters. In practice, we recommend to test extensively in simulation to estimate a possible value of parameters $\bar{u}_k$.

Remark 2. In light of the observations in Remark 1, we recommend to select the values of δ_1 and δ_2 after extensive simulation tests.

References

[1]Silva, N., Martel, F., and Delpy, P., "Automated Transfer Vehicle Thrusters Selection and Management Function," *6th International ESA Conference on Guidance, Navigation and Control Systems*, 2005.

[2]Souza, C. D., Hannak, C., Spehar, P., Clark, F., and Jackson, M., "Orion Rendezvous, Proximity Operations and Docking Design and Analysis," *AIAA Guidance, Navigation and Control Conference and Exhibit*, 2007.

[3]Wie, B., *Space Vehicle Dynamics and Control, Second Edition*, AIAA, 2008.

[4]Agrawal, B. N. and Bang, H., "Robust Closed-Loop Control Design for Spacecraft Slew Maneuver Using Thrusters," *Journal of Guidance, Control, and Dynamics*, Vol. 18, No. 6, 1995, pp. 1336–1344.

[5]Burdick, G. M., Lin, H.-S., and Wong, E. C., "A Scheme for Target Tracking and Pointing During Small Celestial Body Encounters," *Journal of Guidance, Control, and Dynamics*, Vol. 7, No. 4, 1984, pp. 450–457.

[6]Bryson, A. and Ho, Y., *Applied Optimal Control: Optimization, Estimation, and Control*, Hemisphere, New York, 1975.

[7]Rao, V. and Bernstein, D., "Naive Control of the Double Integrator," *IEEE Control Systems*, Vol. 21, No. 5, 2001, pp. 86–97.

[8]Bilimoria, K. D. and Wie, B., "Time-Optimal Three-Axis Reorientation of a Rigid Spacecraft," *Journal of Guidance, Control, and Dynamics*, Vol. 16, No. 3, 1993, pp. 446–452.

[9]Byers, R. M. and Vadali, S. R., "Quasi-Closed-Form Solution to the Time-Optimal Rigid Spacecraft Reorientation Problem," *Journal of Guidance, Control, and Dynamics*, Vol. 16, No. 3, 1993, pp. 453–461.

[10]Bai, X. and Junkins, J. L., "New Results for Time-Optimal Three-Axis Reorientation of a Rigid Spacecraft," *Journal of Guidance, Control, and Dynamics*, Vol. 32, No. 4, 2009, pp. 1071–1076.

[11]Shen, H. and Tsiotras, P., "Time-Optimal Control of Axisymmetric Rigid Spacecraft Using Two Controls," *Journal of Guidance, Control, and Dynamics*, Vol. 22, No. 5, 1999, pp. 682–694.

[12]Krishnan, H., Reyhanoglu, M., and McClamroch, H., "Attitude Stabilization of a Rigid Spacecraft Using Two Control Torques: A Nonlinear Control Approach Based on the Spacecraft Attitude Dynamics," *Automatica*, Vol. 30, No. 6, 1994, pp. 1023–1027.

[13]Singh, S. and Iyer, A., "Nonlinear Decoupling Sliding Mode Control and Attitude Control of Spacecraft," *IEEE Transactions on Aerospace and Electronic Systems*, Vol. 25, No. 5, 1989, pp. 621–633.

[14]Serpelloni, E., Maggiore, M., and Damaren, C. J., "Control of Spacecraft Formations Around the Libration Points Using Electric Motors with One Bit of Resolution," *Journal of the Astronautical Sciences*, 2015.

[15]Serpelloni, E., Maggiore, M., and Damaren, C. J., "Bang Bang Hybrid Stabilization of Perturbed Double Integrators," *53rd IEEE Conference on Decision and Control*, IEEE, 2014.

[16]Serpelloni, E., Maggiore, M., and Damaren, C. J., "Rigid Spacecraft Formations Actuated by Electric Thrusters with One-Bit Resolution," *AIAA/AAS Astrodynamics Specialist Conference*, 2014.

[17]Personne, G., Lopez-Y-Diaz, A., and Delpy, P., "ATV GNC Synthesis: Overall Design, Operations and Main Performances," *6th International ESA Conference on Guidance, Navigation and Control Systems*, 2005.

[18]Amadieu, P., Beckwith, G., Dore, B., Bouchery, J., and Pery, V., "Automated Transfer Vehicle (ATV) Structural and Termal Model at ESTEC," *ESA Bulletin*, No. 111, 2002.

[19]Maggiore, M., Rawn, B., and Lehn, P., "Invariance Kernels of Single-Input Planar Nonlinear Systems," *SIAM Journal on Control and Optimization*, Vol. 50, No. 2, 2012, pp. 1012–1037.